Published in final edited form as:
Biochem Biophys Res Commun. 2011 July 22; 411(1): 69–75. doi:10.1016/j.bbrc.2011.06.090.

An insight into the interaction mode between CheB and chemoreceptor from two crystal structures of CheB methylesterase catalytic domain

Kwang-Hwi Cho[1], **Brian R. Crane**[2], and **SangYoun Park**[1,*]

[1]School of Systems Biomedical Science, Soongsil University, Seoul, Korea

[2]Department of Chemistry and Chemical Biology, Cornell University, Ithaca, New York, USA

Abstract

We have determined 2.2 Å resolution crystal structure of *Thermotoga maritima* CheB methylesterase domain to provide insight into the interaction mode between CheB and chemoreceptors. *T. maritima* CheB methylesterase domain has identical topology of a modified doubly-wound α/β fold that was observed from the previously reported *Salmonella typhimurium* counterpart, but the analysis of the electrostatic potential surface near the catalytic triad indicated considerable charge distribution difference. As the CheB demethylation consensus sites of the chemoreceptors, the CheB substrate, are not uniquely conserved between *T. maritima* and *S. typhimurium*, such surfaces with differing electrostatic properties may reflect CheB regions that mediate protein-protein interaction. *Via* the computational docking of the two *T. maritima* and *S. typhimurium* CheB structures to the respective *T. maritima* and *Escherichia coli* chemoreceptors, we propose a CheB:chemoreceptor interaction mode.

Keywords

CheB; Methylesterase; *Thermotoga maritima*; Chemoreceptor; Methyl-accepting chemotaxis proteins; Protein-protein interaction

Introduction

Bacterial chemotaxis is a signal transduction cascade which allows bacteria to swim towards an attractant or away from a repellent chemical. Bacterial chemotaxis begins in response to the sensing of extracellular chemicals by the membrane-spanning chemoreceptors (also known as methyl-accepting chemotaxis proteins; MCPs), and bacteria use their flagella to either smooth-swim forward, or to tumble resulting in a randomly changing swimming direction. In bacteria such as *Escherichia coli*, the respective smooth-swimming and tumbling behavior is the result of alternation between a counter-clockwise (CCW) and a clockwise (CW) flagellar rotation [1–10]. In *E. coli*, a chemical ligand binding to the

*To whom correspondence should be addressed: SangYoun Park, PhD, School of Systems Biomedical Science, College of Natural Science, Soongsil University, 511 Sangdo-Dong, Dongjak-Gu, Seoul 156-743, Korea, Phone: 82-2-820-0456, Fax: 82-2-824-4383, psy@ssu.ac.kr.

Accession Code: Worldwide Protein Data Bank coordinate for *T. maritima* $CheB_C$ has been deposited with an accession code 3SFT.

extracellular domain of the chemoreceptor is transmitted to the cytoplamsic CheA kinase, thus triggering kinase activity. CheA-bound ATP is auto-phosphorylated to a histidine of CheA, and is subsequently transferred to an aspartate of the two response-regulators, CheY and CheB. CheY and CheB bind competitively to CheA [11], and consequently determine two responses: “excitation” and “adaptation”. In the “excitation” process mediated by CheY, phospho-CheY detaches from CheA to interact with the switch protein FliM at the flagellar motor complex, which alters the rotational direction of the flagella.

However, after the CheY-mediated response, bacteria return to the pre-stimulus state *via* a slower “adaptation” process mediated by CheB. Adaptation can be viewed as a negative feedback mechanism that allows the bacteria to detect temporally increasing gradients of chemicals, by preventing saturation. In general, two chemoreceptor modifying enzymes - CheR and CheB - each catalyze the methylation and demethylation of glutamates in the chemoreceptors, and the level of reversible methylation during the “adaptation” behavior enables the chemoreceptor’s attenuated sensitivity to the ligand. Methyltransferase CheR constantly methylates the chemoreceptors *via* S-adenosyl-L-methionine, and methylesterase CheB functions in accordance with the activated CheA. CheB binds to CheA *via* an N-terminal CheY-like response-regulator domain which becomes phosphorylated by CheA. As is seen in CheY after CheA phosphorylation, phospho-CheB detaches from CheA, resulting in a concomitant opening of the C-terminal catalytic domain ($CheB_c$) for catalytic methylesterase activity [12–15]. The activated $CheB_c$ subsequently hydrolyzes the methyl glutamates of the chemoreceptor, and results in the deactivation of the chemoreceptor, thus setting a new threshold compared to the previous chemical concentration.

Glutamates that undergo CheR-mediated methylation and CheB-mediated demethylation are located at the cytoplasmic regions of the membrane-spanning chemoreceptors. The CheR-mediated methylation consensus sites have been defined for chemoreceptors of *Salmonella enterica* Tar [16] and *E. coli* Tsr [17], and the protein-protein interaction surface harboring the glutamate methylation sites has been predicted *via* docking studies [18] using the structures of the *E. coli* Tsr chemoreceptor (PDB code: 1QU7) [19] and CheR (PDB code: 1BC5) [20]. A recent study has also defined the CheR-mediated methylation consensus sites of *Thermotoga maritima* chemoreceptors, and the results demonstrate that the sites are not uniquely conserved between distant bacterial species of *S. enterica* or *E. coli* [22].

Despite the known crystal structures of full-length *Salmonella typhimurium* CheB (PDB code: 1A2O) [15] and $CheB_c$ (PDB code: 1CHD) [21], only limited attempts have been made to model the $CheB_c$ and the chemoreceptor interaction. Provided that the interaction modes are conserved between distant bacterial species, an improved model may be generated by comparing the docking results from more than two sets of interacting protein pairs. For this approach, we have determined the crystal structure of *T. maritima* $CheB_c$, and by using this structure together with the structures of *S. typhimurium* $CheB_c$ [15, 21], *T. maritima* chemoreceptor [23] and *E. coli* chemoreceptor [19], we propose a $CheB_c$ and chemoreceptor interaction model.

Materials and methods

Protein Preparation

The genes encoding *T. maritima* methylesterase domain of CheB ($CheB_c$: residues 153–344) were PCR cloned into the vector pET28a (Novagen) using the *T. maritima* genomic DNA (ATCC). The protein was expressed with N-terminal His_6-tag in *E. coli* strain BL21 (DE3) (Stratagene) using kanamycin selection (25 μg/mL). Using a conventional shaker, the transformed cells were grown at 37 °C in 2 L of Terrific Broth medium to OD_{600}= ~0.6. The recombinant protein expression was induced with 0.5 mM isopropyl β-D-

thiogalactopyranoside (IPTG), and the cells were further grown at 25 °C for 16 hrs. The cell pellets were harvested using centrifugation at 4500 g for 10 mins at 4°C, and were re-suspended in ice-cold lysis buffer (20 mM TRIS pH 7.5, 500 mM sodium chloride and 5 mM imidazole) prior to homogenization by sonication.

The cell lysate was centrifuged at 70000g for 30 mins at 4°C. The supernatants were loaded onto Nickel-NTA columns, washed with wash buffer (20 mM TRIS pH 7.5, 500 mM sodium chloride and 20 mM imidazole) and the recombinant proteins were eluted with elution buffer (20 mM TRIS pH 7.5, 500 mM sodium chloride and 200 mM imidazole). The His_6-tag was removed by treating the eluted protein with human thrombin (Roche) for 16 hrs at 4°C. The protein was further purified using a Superdex 200 sizing column (GE Healthcare) equilibrated in gel-filtration buffer (50 mM TRIS pH 7.5 and 150 mM NaCl). The eluting fractions corresponding to $CheB_c$ were concentrated to ~50 mg/mL by centrifugation (Amicon Millipore). Protein purity determined on SDS-PAGE was >95% and the concentration was estimated by absorption at λ=280 nm by employing the calculated molar extinction coefficient of 7680 M^{-1} cm^{-1} (SWISS-PROT; http://www.expasy.ch/).

Crystallization and Data Collection

Conditions for growing *T. maritima* $CheB_c$ crystals were found in commercial screening solutions (Hampton Research). Crystallization screenings were performed at 25 °C by using hanging drop vapor diffusion method where the protein and the well solutions were mixed in 1:1 ratio of total 2 μL volumes. Diffraction quality crystals grew after two months against a reservoir of 0.2 M ammonium sulfate, 0.1 M cacodylate pH 6.5 and 30% (w/v) PEG 8K. Diffraction data were collected under a 100 K nitrogen stream at a NSLS beamline (X25) on a CCD detector (ADSC Quantum 315). The crystal belongs to the space group $P2_12_12_1$ and contains one molecule per asymmetric unit. Data were processed by DENZO and SCALEPACK [24].

Structure determination and refinement

The position of $CheB_c$ was determined by AMoRe molecular replacement [25] with free catalytic domain of *S. typhimurium* CheB as a search model (PDB code: 1CHD) and the diffraction data of 4.0 – 10.0 Å resolution. The entire model of $CheB_c$ was automatically built with ARP/wARP and SIDEgui [26] in CCP4 suite [27]. The final model (one $CheB_c$ molecule in asymmetric unit, residues 156–344) was further refined in CNS (R-factor = 0.204, R_{free} = 0.223 where R_{free} is the R-factor for 10% of randomly selected reflections excluded from the refinement.) [28].

Computational modelling of CheB and chemoreceptor interaction

The structures of the *S. typhimurium* CheB methylesterase domain (PDB code: 1CHD) and the *E. coli* chemoreceptor Tsr (PDB code: 1QU7; edited only to include α-helices containing the methylation Glu/Gln of residues 294-320 and 464-493 in each subunit), both lacking all heteroatoms, were docked using the ZDOCK program [29]. This program carries out rigid-body docking at all possible orientations between the two proteins, $CheB_c$ and Tsr. Among them, 1,000 predicted complexes were selected based on the scoring function implemented in the program. The RDOCK program [30] was used for refinement and energy minimization of the complexes with a CHARMM force field [31]. The docked complexes were ranked based on the shape complementarities and electrostatic considerations implemented in the program, and only the top 40% were considered for the subsequent filtering processes. The top 40% complexes were filtered further on the basis of the constraints of the distance measured from three residues of the CheB catalytic triad (Ser164, His190 and Asp286) and each of the methylation Glu/Gln residues (Gln297, Glu304, Gln311). Cα-to-Cα distance constraints of at least one triad residue to Glu (or Gln) within 9

Å, and the sum of three triad residues to Glu (or Gln) within 32 Å were applied. This filtering step yielded two complexes for the methylation site Gln297, two complexes for site Glu304, and six complexes for site Gln311.

Similar steps were applied for the docking of *T. maritima* $CheB_c$ and the *T. maritima* chemoreceptor TM1143 (PDB code: 2CH7; edited to only to include α-helices containing the methylation Glu/Gln of residues 262-297 and 454-489 in each subunit). The two structures were docked using ZDOCK and minimized with RDOCK. The docked complexes were ranked and only the top 40% were considered for the subsequent filtering process by Cα-to-Cα distance. Distance constraints were based on the distance measured from three residues of the CheB catalytic triad (Ser166, His193 and Asp289) and each of the methylation Glu/Gln residues (Gln281 and Glu294). Cα-to-Cα distance constraints of at least one triad residue to Glu/Gln within 10 Å, and the sum of three triad residues to Glu-Gln within 30 Å were applied. This filtering step yielded only two complexes (no. 400 and no. 554) for the Gln281 methylation site. The 10 complexes resulting in the case of *E. coli* (or *S. typhimurium*) proteins and two complexes for the *T. maritima* proteins were assessed and compared using the PyMol molecular graphics display program [31]. All the structural figures were also rendered with PyMol [32].

Results and Discussion

Overall structure of T. maritima $CheB_c$

The crystal structure of *T. maritima* CheB methylesterase domain was determined to a resolution of 2.2 Å using a *S. typhimurium* CheB structure (PDB code: 1CHD) as a molecular replacement model. The refined model harbours one α/β sandwich-fold $CheB_c$ molecule within the crystal asymmetric unit, which is composed of nine β-strands, six α-helices, and one 3_{10}-helix (Fig. 1). Among the 192 residues designed in the protein construct, 189 residues were built in the model. The three N-terminal CheB residues (153-KPA-155) were not included in the model, as their electron densities were not clearly discernable. 106 water molecules were also included. Data collection and refinement statistics are provided in Table 1 and Table 2.

The fold of *T. maritima* $CheB_c$ is identical to that of *S. typhimurium* $CheB_c$, which is a modified, doubly wound α/β fold containing the central seven parallel β-strands flanked by six α-helices and an anti-parallel β-hairpin (Fig. 2). In brief, the fold starts from β1 and the subsequently alternating α-helices and β-strands (α1-β2/α2-β3/β4) form one core of the central parallel β-sheet (β1/β2/β4/β3). The following two β-strands (β5-β6) form an anti-parallel β-hairpin distal to the central parallel β-sheet, which result in a modified α/β fold. Finally, the three following sets of alternating α-helix and the β-strand (α3-β7/α4-β8/α5-β9) complete the second half of the central seven-stranded β-sheet (β9/β8/β7/β1/β2/β4/β3). The catalytic Ser-His-Asp triad which generates the methylesterase activity lie at the surface created mainly by loops that connect the β-strands and the α-helices (β1-α1 loop, β2-α2 loop, β6-α3 loop, β7-α4 loop). Two other loops (β3-β4 and 3_{10} helix-α5 loop) are also in the vicinity of the catalytic triad (Fig. 2).

Surface electrostatic potential difference between T. maritima and S. typhimurium $CheB_c$

As *T. maritima* and *S. typhimurium* $CheB_c$s are conserved with 36% identity (54% similarity) in their protein sequences (Fig. 1), the superposition of *T. maritima* and *S. typhimurium* $CheB_c$s (PDB code: 1CHD) is clearly indicative of an overlap of secondary structural elements (C_α RMSD=1.032 Å aligning 182 residues). Partial sequence conservation also occurs near the catalytic surface of the protein, which is created by the contiguous loops that connect the β-strands and the α-helices (Fig. 1, β1-α1 loop, β2-α2

loop, β6-α3 loop, β7-α4 loop). However, analysis of the electrostatic potential surface near the catalytic triad reflects considerable differences in the charge distribution between the two *T. maritima* and *S. typhimurium* $CheB_c$s. The region of conspicuous differences is outlined along the arrows near the catalytic triad surface (Fig. 2C).

The CheR-mediated methylation consensus sites neighboring the modified glutamate have been defined for chemoreceptors of *S. enterica* Tar [17], *E. coli* Tsr [16], and several *T. maritima* chemoreceptors [22], and the results demonstrate that the sites are not uniquely conserved. As perfect complementarity of proteins, the fundamental driver of biological specificity, within biologically relevant complexes results during and requires co-evolution [33], such surfaces with differing electrostatic properties may reflect $CheB_c$ regions that mediate interactions with chemoreceptors.

Methylation-undergoing glutamates of chemoreceptors, which are also the substrates for methylesterase CheB, are located in the cytoplasmic regions of the membrane-spanning chemoreceptor. The methylation (or demethylation) consensus sequences (Glx-**Glx**-X-X-Ala-Ser/Thr, methylation residue is in bold) of *S. enterica* (Tar) and *E. coli* (Tsr) chemoreceptors [16, 17] have been shown to differ slightly from that of the *T. maritima* receptors (Ala/Ser-sm-X-**Glx-Glu**-X-sm-Ala/Ser, methylation residues are in bold; sm indicates small residues which are either Ala, Gly, Ser or Thr) [22]. Two $CheB_c$s recognizing the different consensus sequence of the chemoreceptors can be mapped to the different surface complementarities which have co-evolved between the chemoreceptor substrate and the CheB enzyme. Electrostatic potential surfaces near the *T. maritima* and *S. typhimurium* $CheB_c$ catalytic triad with substantial differences suggested that two $CheB_c$ structures in conjunction with the chemoreceptor's structural information may assist in generating a reliable CheB and chemoreceptor interaction model. A systematic docking study has been carried out using two sets of $CheB_c$ and chemoreceptor structures originating from *T. maritima* and *S. typhimurium*. Provided that the general interaction modes are conserved between the two distant bacterial species, an interaction model has been generated by comparing the overlapping docking results.

Prediction of chemoreceptor and CheB interaction mode

E. coli and *S. typhimurium* both belong to the Enterobacteriaceae family and are closely related in the bacterial phylogeny tree. As the CheBs from the two species also share 95% sequence identity, the structures of the cytoplasmic regions of the *E. coli* Tsr chemoreceptor (PDB code: 1QU7) and *S. typhimurium* $CheB_c$ (PDB code: 1CHD) were docked using ZDOCK and RDOCK. Docking was carried out solely using the truncated four-helix bundle of the chemoreceptor, which includes the methylation Glu/Gln (Gln297, Glu304, and Gln311). The docking results were sorted on the basis of the relevant complementarities and electrostatic considerations, and further filtered using distance constraints between the catalytic residues and methylation glutamates. The final result yielded 10 $CheB_c$ and chemoreceptor complexes in three Tsr methylation Glu/Gln residues (two complexes for site Gln297, two complexes for site Glu304, and six complexes for site Gln311). However, when the 10 complexes were superposed relative to $CheB_c$, the positions of the chemoreceptor relative to $CheB_c$ - i.e. the directionality of the chemoreceptor four-helix bundle - in the 10 complexes were heterogeneous, which indicates that generating a single interaction mode is not possible (results not shown).

Similar docking steps were applied for the case of *T. maritima* $CheB_c$ and the TM1143 chemoreceptor (PDB code: 2CH7). A recently reported cytoplasmic structure of the *T. maritima* chemoreceptor TM0014 (PDB code: 3G67) [34] was not included in the docking set due to the absence of the methylation consensus sequences. Similar to the previous case, docking was carried out solely using the truncated four-helix bundle of the chemoreceptor

which includes the methylation Glu/Gln (Gln294 and Gln281). After sorting and filtering processes using distance constraints, the final docking result with the *T. maritima* proteins yielded two $CheB_c$ and chemoreceptor complexes (no. 400 and no. 554) around only the Gln281 methylation residue. The positions of the chemoreceptor relative to $CheB_c$ in the two resultant complexes are practically identical, with only a slight ~1° shift in the four-helix bundle around Gln281 (results not shown). When the two docking complexes from *T. marimita* proteins were overlaid with the 10 docking complexes from *E. coli* proteins, only one *E. coli* docking pair (no. 640 from site Gln311) matched exactly with an identical helical arrangement of the chemoreceptor substrate relative to $CheB_c$ (Fig. 3). Surprisingly, when the α-helix of the chemoreceptor containing the demethylation site was observed outside the context of the four-helix bundle, it sits within a groove created at the adjunction of the four $CheB_c$ α-helices (α1, α2, α3, and α4, Fig. 4). The interaction surface is created by the contacting loops that connect the β-strands to the α-helices (β1-α1 loop, β2-α2 loop, β6-α3 loop, β7-α4 loop), and is the region where majority of the electrostatic potential surface differed between the two *T. maritima* and *S. typhimurium* $CheB_c$s (Fig. 2C & Fig. 4). It is worth noting that this $CheB_c$ groove has also been previously predicted to be the chemoreceptor interface, which was concluded from the manual inspection of a 10 Å - diameter channel that accommodates an α-helix [21].

We have succeeded in generating a probable model between the two interacting proteins using the systematic docking approach that defines the helical orientation of the chemoreceptor relative to $CheB_c$. However, since *T. maritima* CheB demethylates on at least two different methyl glutamates of the chemoreceptor, more than one interaction mode – an interface covering methylation residues Gln294 as well as Gln281 – should be predicted from the docking methods. As no docking results satisfy the constraints on Gln294, we are unable to suggest multiple modes of $CheB_c$ interaction between the different demethylation glutamates.

In summary, we have determined the crystal structure of *T. maritima* $CheB_c$ and used it to generate a chemoreceptor interaction model by carrying out docking studies. We have clearly demonstrated that the limited efficiencies of the docking processes can be enhanced in cases in which two or more structure sets of interacting proteins are known from different species. Although we had aimed to crystallize *T. maritima* $CheB_c$ in complex with the TM1143 chemoreceptor, to date this has not proven successful. A more complete picture of methylesterase $CheB_c$ and the chemoreceptor substrate interaction thus awaits a successful determination of the complex structure.

Acknowledgments

This work was supported by the Human Resources Development of the Korea Institute of Energy Technology Evaluation and Planning (KETEP) grant funded by the Ministry of Knowledge Economy, Republic of Korea (No. 20104010100610) to K.W.C., and NIH grant GM066775 to B.R.C. This work was supported by the Research carried out (in part) at the National Synchrotron Light Source, Brookhaven National Laboratory, which is supported by the U.S. Department of Energy, Division of Materials Sciences and Division of Chemical Sciences, under Contract No. DE-AC02-98CH10886. We thank J. Y. Park for graphical assistance during figure preparation.

References

1. Borkovich KA, Simon MI. The dynamics of protein phosphorylation in bacterial chemotaxis. Cell. 1990; 63:1339–1348. [PubMed: 2261645]
2. Parkinson JS, Kofoid EC. Communication modules in bacterial signaling proteins. Annu Rev Genet. 1992; 26:71–112. [PubMed: 1482126]
3. Appleby JL, Parkinson JS, Bourret RB. Signal transduction via the multistep phosphorelay: not necessarily a road less travelled. Cell. 1996; 86:845–848. [PubMed: 8808618]

4. Goudreau PN, Stock AM. Signal transduction in bacteria: molecular mechanisms of stimulus-response coupling. Curr Opin Microbiol. 1998; 1:160–169. [PubMed: 10066483]
5. Berg HC. The rotary motor of bacterial flagella. Annu Rev Biochem. 2003; 72:19–54. [PubMed: 12500982]
6. Kojima S, Blair DF. The bacterial flagellar motor: structure and function of a complex molecular machine. Int Rev Cytol. 2004; 233:93–134. [PubMed: 15037363]
7. Wadhams GH, Armitage JP. Making sense of it all: bacterial chemotaxis. Nat Rev Mol Cell Biol. 2004; 5:1024–1037. [PubMed: 15573139]
8. Sourjik V. Receptor clustering and signal processing in E. coli chemotaxis. Trends Microbiol. 2004; 12:569–576. [PubMed: 15539117]
9. Parkinson JS, Ames P, Studdert CA. Collaborative signaling by bacterial chemoreceptors. Curr Opin Microbiol. 2005; 8:116–121. [PubMed: 15802240]
10. Inouye, M.; Dutta, R. Histidine Kinases in Signal Transduction. Academic Press; San Diego: 2002.
11. Li J, Swanson RV, Simon MI, Weis RM. The response regulators CheB and CheY exhibit competitive bind to the kinase CheA. Biochemistry. 1995; 34:14626–14636. [PubMed: 7578071]
12. Lupas A, Stock J. Phosphorylation of an N-terminal regulatory domain activates the CheB methylesterase in bacterial chemotaxis. J Biol Chem. 1989; 264:17337–17342. [PubMed: 2677005]
13. Stewart RC. Activating and inhibitory mutations in the regulatory domain of CheB, the methylesterase in bacterial chemotaxis. J Biol Chem. 1993; 268:1921–1930. [PubMed: 8420965]
14. Anand GS, Goudreau PN, Stock AM. Activation of methylesterase CheB: Evidence of a dual role for the regulatory domain. Biochemistry. 1998; 37:14038–14047. [PubMed: 9760239]
15. Djordjevic S, Goudreau PN, Xu Q, Stock AM, West AH. Structural basis for methylesterase CheB regulation by a phosphorylation-activated domain. Proc Natl Acad Sci USA. 1998; 95:1381–1386. [PubMed: 9465023]
16. Terwilliger TC, Koshland DE Jr. Sites of methyl esterification and deamination on the aspartate receptor involved in chemotaxis. J Biol Chem. 1984; 259:7719–7725. [PubMed: 6330075]
17. Kehry MR, Bond MW, Hunkapiller MW, Dahlquist FW. Enzymatic deamidation of methyl-accepting chemotaxis proteins in Escherichia coli catalyzed by the cheB gene product. Proc Natl Acad Sci U S A. 1983; 80:3599–3603. [PubMed: 6304723]
18. Perez E, West AH, Stock AM, Djordjevic S. Discrimination between different methylation states of chemotaxis receptor Tar by receptor methyltransferase CheR. Biochemistry. 2004; 43:953–961. [PubMed: 14744139]
19. Kim KK, Yokota H, Kim SH. Four-helical-bundle structure of the cytoplasmic domain of a serine chemotaxis receptor. Nature. 1999; 400:787–792. [PubMed: 10466731]
20. Djordjevic S, Stock AM. Chemotaxis receptor recognition by protein methyltransferase CheR. Nat Struct Biol. 1998; 5:446–450. [PubMed: 9628482]
21. West AH, Martinez-Hackert E, Stock AM. Crystal structure of the catalytic domain of the chemotaxis receptor methylesterase, CheB. J Mol Biol. 1995; 250:276–290. [PubMed: 7608974]
22. Perez E, Zheng H, Stock AM. Identification of methylation sites in Thermotoga maritima chemotaxis receptors. J Bacteriol. 2006; 188:4093–4100. [PubMed: 16707700]
23. Park S-Y, Borbat PR, Gonzalez-Bonet G, Bhatnagar J, Pollard AM, Freed JH, Bilwes AM, Crane BR. Reconstruction of the chemotaxis receptor-kinase assembly. Nat Struct Mol Biol. 2006; 13:400–407. [PubMed: 16622408]
24. Otwinowski Z, Minor W. Processing of X-ray diffraction data in oscillation mode. Methods Enzymol. 1997; 276:307–325.
25. Navaza J. *AMoRe*: an automated package for molecular replacement. Acta Cryst. 1994; A50:157–163.
26. Perrakis A, Morris RM, Lamzin VS. Automated protein model building combined with iterative structure refinement. Nat Struct Biol. 1999; 6:458–463. [PubMed: 10331874]
27. Collaborative Computational Project Number 4, The CCP4 suite: programs for protein crystallography. Acta Cryst. 1994; D50:760–763.

28. Brünger AT, Adams PD, Clore GM, DeLano WL, Gros P, Grosse-Kunstleve RW, Jiang JS, Kuszewski J, Nilges M, Pannu NS, Read RJ, Rice LM, Simonson T, Warren GL. Crystallography and NMR system: a new software suite for macromolecular structure determination. Acta Crystallogr D Biol Crystallogr. 1998; 54:905–921. [PubMed: 9757107]

29. Chen R, Li L, Weng Z. ZDOCK: an initial-stage protein-docking algorithm. Proteins. 2003; 52:80–87. [PubMed: 12784371]

30. Li L, Chen R, Weng Z. RDOCK: refinement of rigid-body protein docking predictions. Proteins. 2003; 53:693–707. [PubMed: 14579360]

31. Brooks BR, Bruccoleri RE, Olafson BD, States DJ, Swaminathan S, Karplus M. CHARMM: A program for macromolecular energy, minimization, and dynamics calculations. J Comput Chem. 1983; 4:187–217.

32. DeLano, WL. The PyMOL Molecular Graphics System. DeLano Scientific; San Carlos, CA, USA: 2002. http://www.pymol.org

33. Park SY, Jin W, Woo JR, Shoelson SE. Crystal structures of Human TBC1D1 and TBC1D4 (AS160) RabGAP domains reveal critical elements for GLUT4 translocation. J Biol Chem. 2011; 286:18130–18138. [PubMed: 21454505]

34. Pollard AM, Bilwes AM, Crane BR. The structure of a soluble chemoreceptor suggests a mechanism for propagating conformational signals. Biochemistry. 2009; 48:1936–1944. [PubMed: 19149470]

- We report the structure of *T. maritima* CheB methylesterase domain.
- We have compared the structure with the *S. typhimurium* CheB.
- Analysis indicates differing electrostatic surfaces near the catalytic region.
- We carry out computational docking using the two respective chemoreceptor structures.
- We thereby propose a CheB:chemoreceptor interaction mode.

Figure 1. Sequence alignment of $CheB_c$ from five organisms

$CheB_c$ sequences from *T. maritima*, *E. coli*, *S. typhimurium*, *Bacillus subtilis* and *Myxococcus xanthus* were aligned on the basis of the amino acid sequences. Secondary structural elements are indicated as block rectangles (α-helix) and arrows (β-sheet) on top of the corresponding amino acid residues. Conserved residues are boxed around the amino acids. Catalytically critical residues (Ser-His-Asp triad) are indicated with an asterisk.

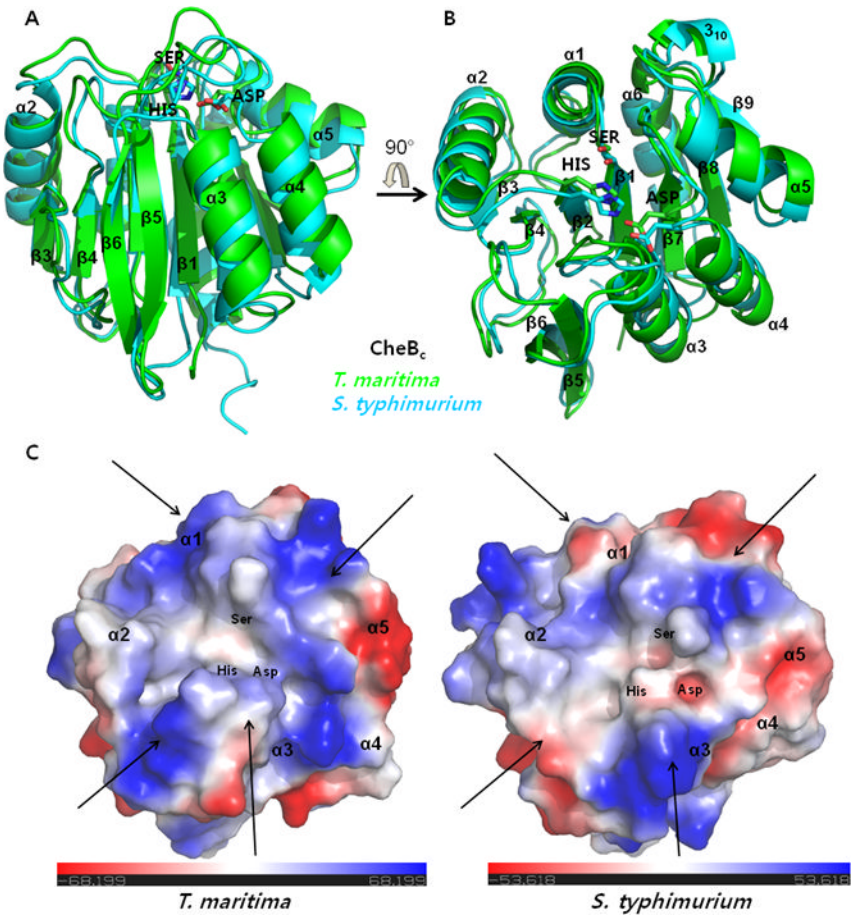

Figure 2. Similarities in the overall fold do not account for the dissimilarities in the electrostatic potential surface of *T. maritima* and *S. typhimurium* $CheB_C$

(A, B) Schematic ribbon diagrams of the superimposed structures of *T. maritima* and *S. typhimurium* $CheB_C$ are shown in two different orientations which are rotated 90° with respect to each other along the horizontal arrow. Three side chains of the catalytic triad are shown in sticks. (C) Differences in the electrostatic potential surface near the catalytic triad are highlighted using colors by charge. The surface was generated from the 90°-rotated orientation (B) which looks at the catalytic triad from the top. Dissimilar regions of charge distribution in *T. maritima* and *S. typhimurium* are mostly located around regions indicated with arrows. Since the consensus sequences adjacent to the methylation/demethylation glutamates of the chemoreceptors are not exactly conserved between the two species, such surface with electrostatic difference may be the sites of chemoreceptor interaction.

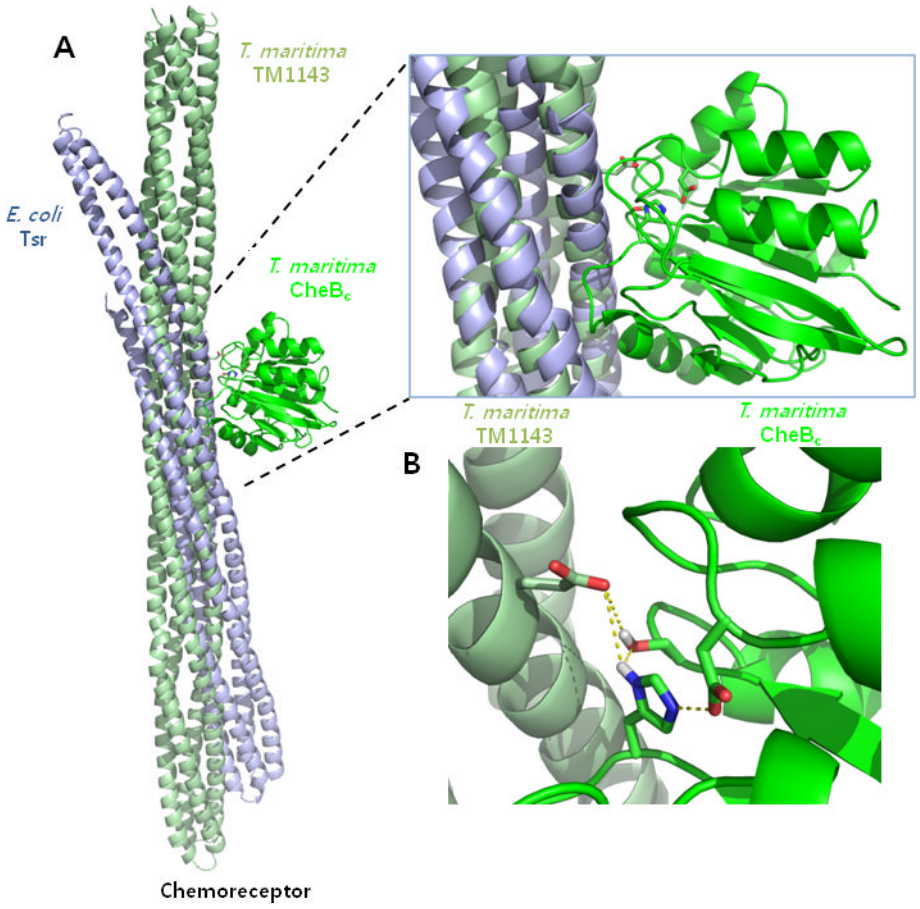

Figure 3. Proposed chemoreceptor docking site for *T. maritima* and *S. typhimurium* $CheB_c$

(A) Docking models were generated from the PDB coordinates of the chemoreceptors and the $CheB_c$s from *T. maritima* and *S. typhimurium* using ZDOCK and RDOCK. Overall docking modes are shown with the chemoreceptor positions relative to the superimposed $CheB_c$ (Only *T. maritima* $CheB_c$ is shown for clarity). (B) The methylation residue for the *T. maritima* chemoreceptor (Gln281) is shown with sticks in relation to the catalytic triad. Distances indicate the measured bonding distance between atoms in the model.

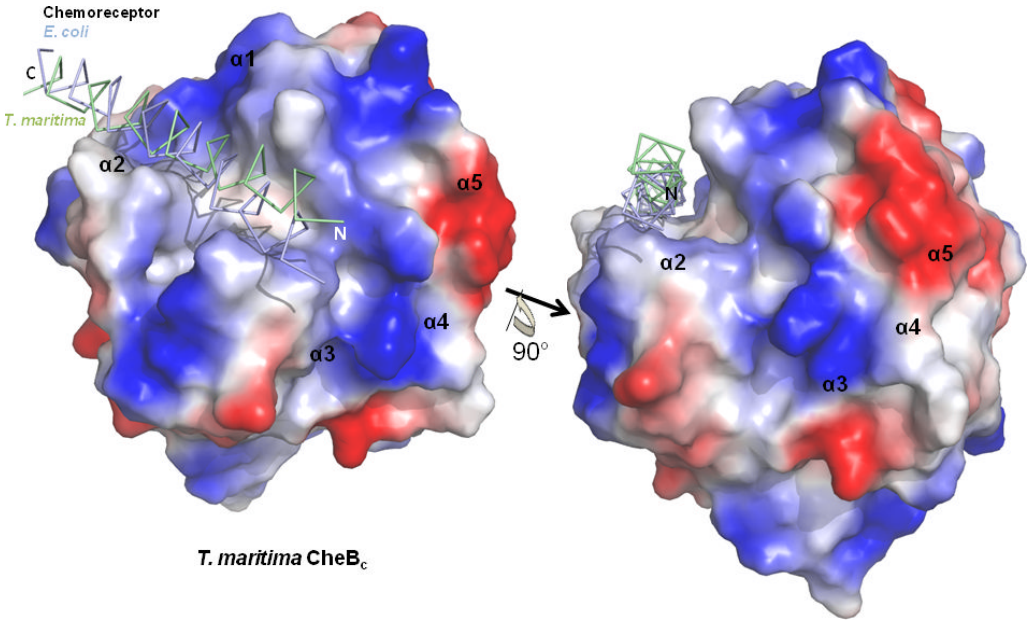

Figure 4. View of the proposed docking site with chemoreceptor α-helix shown over the *T. maritima* $CheB_c$ electrostatic potential surface

View of the truncated α-helical substrate of the *T. maritima* and *E. coli* chemoreceptor overlaid on top of the *T. maritima* $CheB_c$ electrostatic potential surface are shown in two different orientations, which are rotated 90° with respect to each other along the indicated axis (Only *T. maritima* $CheB_c$ is shown for clarity). The α-helical substrate of the chemoreceptor sits within a groove created at the active site.

Table 1

Data Collection and Phasing Statistics

Wavelength(Å)	1.100
Resolution(Å)	30–2.15
Highest Shell	(2.23–2.15)
Completeness (%)	99.9(99.9)
R_{merge}[1]	0.106(0.382)
I/σ(I)	35(8.4)

[1] $R_{merge} = \Sigma\Sigma_j |I_j - \langle I \rangle| / \Sigma\Sigma_j I_j$

Table 2

Refinement Statistics

Space Group	$P2_12_12_1$ (a= 52.47 Å, b=65.08 Å, c=78.35 Å)
Resolution range (Å)	30–2.2
Unique Reflections (test set)	13555(1382)
Wilson B ($Å^2$)	28.51
R-factor[1] (R_{free}[2])	0.204 (0.223)
No. of Scatters (No. of residues)	2928(189)
No. of Water molecules	106
RMSD bonds (Å)	0.00624
RMSD angles(°)	1.405
Average B-factor (main chain) ($Å^2$)	24.29
Average B-factor (side chain) ($Å^2$)	26.40
Average B-factor (water) ($Å^2$)	38.31

[1] R-factor = $\Sigma(|F_{obs}|-|F_{calc}|)/\Sigma|F_{obs}|$

[2] R-factor for 10% of randomly selected reflections excluded from the refinement.